Chemical Engineering Journal 161 (2010) 212–222

Contents lists available at ScienceDirect

Chemical Engineering Journal

journal homepage: www.elsevier.com/locate/cej

Acid exchange resins deactivation in the esterification of free fatty acids

Riccardo Tesser[a], Martino Di Serio[a], Luca Casale[a], Lucio Sannino[b], Marianna Ledda[b], Elio Santacesaria[a,*]

[a] University of Naples Federico II, Department of Chemistry, via Cintia 80126, Naples, Italy
[b] ASER S.r.l. Co, via F. Icace n.1, 84131, Salerno, Italy

ARTICLE INFO

Article history:
Received 8 January 2010
Received in revised form 16 March 2010
Accepted 14 April 2010

Keywords:
Esterification
Ion-exchange resins
Deactivation
Free fatty acids
Biodiesel

ABSTRACT

In this work the deactivation of an ionic exchange resin, used as catalyst for promoting the esterification of fatty acids for producing biodiesel, has been studied. At this purpose, a dynamic mathematical model, suitable to describe the performances of a continuous tubular reactor containing the catalysts mixed with stainless steel springs as inert diluent, and its evolution with time due to the catalyst deactivation, has been developed. Experimental runs, performed in a pilot plant tubular reactor on fatty acid mixtures (oleins), are reported in the paper. The catalyst deactivation has been shown to depend mainly on the poisoning effect of iron that was present as impurity in the fatty acids used as feedstock. Some information about catalyst regeneration is also given at the end of the paper.

1. Introduction

The worldwide interest towards biofuels has recently grown significantly as a direct result of the renewed need of facing the global warming effect by reducing the greenhouse gases emissions that are related to the wide use of fossil fuels. With this respect, biodiesel represents a valuable alternative to petroleum-derived fuels due to both its renewable nature and its substantially null net carbon dioxide emission. Biodiesel is normally produced by transesterification of highly refined vegetal oils with methanol in the presence of homogeneous alkaline catalysts like sodium or potassium hydroxide or related alkoxides [1,2]. The use of the mentioned alkaline catalysts is not compatible with the presence of free fatty acids and moisture, because, the formation of soaps determining long settling time for separating biodiesel from the by-product glycerol. This is a drawback of this technology because many cheaper feedstock like waste or fried oils cannot be used for producing biodiesel. As a matter of fact, with the current technology the cost of biodiesel is affected for more than 85% by the feedstock supply [3]. At this purpose, new technologies have recently been proposed like: the use of supercritical methanol [4] and a two-stage process (esterification + transesterification) [5,6]. Esterification of free fatty acids (FFA) can be promoted by Broensted acid catalysts, both homogeneous [5,6] and heterogeneous. Many different heterogeneous acid catalysts have been proposed for this reaction but one of the most studied and used is the sulphonic acid exchange resin [7]. A recent review on the use and properties of exchange resins has been published by Alexandratos [8]. The exchange resins are subjected to remarkable swelling [9–12] in the presence of polar substances. This phenomenon must be carefully considered in a kinetic approach for either the liquid volume absorbed or the selectivity in absorption. The liquid composition inside an exchange resin particle could be quite different with respect to the liquid bulk. This is particularly true for the binary mixture water–methanol.

We have studied the importance of this aspect in a previous work [12] where we have shown the effect of neglecting the partition equilibria for runs performed in the presence of different amounts of catalyst. As water is more retained by the resin than methanol, the use of a greater amount of catalyst has the consequence of altering the reaction rate inside the particles. This aspect becomes dramatic in packed bed pilot plant reactor where the catalyst concentration is very high.

A first paper published by Tesser et al. [13] reported a simplified kinetics of the esterification reaction of oleic acid with methanol in the presence of triglycerides, catalyzed by an acid exchange resin in a batch reactor. Furthermore, Santacesaria et al. [14,15] have shown that the esterification reaction, performed in a continuous packed bed tubular reactor (PBR), is possible but, in order to achieve high conversions, a long residence times and consequently low volumetric flow rates are required resulting in very low Reynolds numbers at which the external fluid-to-solid mass transfer resistance becomes significant in comparison with the intrinsic kinetics. Tesser et al. [16] have shown that the kinetic regime can be reached by conducting the esterification reaction in a packed bed loop reactor (PBLR) operated in batch conditions. By adopting a sufficiently high recirculation flow rate, as expected, the PBLR operates near to

* Corresponding author. Tel.: +39 081 674027; fax: +39 081 674026.
E-mail address: elio.santacesaria@unina.it (E. Santacesaria).

1385-8947/$ – see front matter © 2010 Elsevier B.V. All rights reserved.
doi:10.1016/j.cej.2010.04.026

Nomenclature

Ac	acidity wt% in oleic acid
a_s	specific interface area ($cm^2\ cm^{-3}$)
C	concentration ($mol\ mL^{-1}$)
C_{cat}	concentration of catalyst ($g_{cat}\ mL^{-1}$)
C_{Fe}	iron concentration ($mmol\ mL^{-1}$)
C_{titr}	concentration of titrant ($mol\ mL^{-1}$)
C_σ	concentration of active sites ($meqH^+\ g_{cat}{}^{-1}$)
d_p	particles average diameter (cm)
D_{eff}	effective diffusivity ($cm^2\ min^{-1}$)
E_A	activation energy ($kcal\ mol^{-1}$)
H	ionic exchange equilibrium constant
k	kinetic constant of uncatalyzed reaction ($mL^2\ mol^{-2}\ min^{-1}$)
k_{cat}, k_{-cat}	kinetic constants of the forward and the reverse reaction ($mL^{-1}\ g_{cat}{}^{-1}\ min^{-1}$)
k_d	deactivation kinetic constant ($g_{cat}\ mL\ min^{-1}\ meqH^{+\ -2}$)
k_S	mass transfer coefficient ($cm\ min^{-1}$)
K	partition constant ($mL\ mol^{-1}$)
K^{eff}	effective partition constant
m_{sample}	weight of sample (g)
M	molecular weight ($g\ mol^{-1}$)
n	number of moles (mol)
N	number of experimental data
Q	volumetric flow rate ($mL\ min^{-1}$)
r_{cat}	rate of catalyzed reaction ($mol\ min^{-1}\ g_{cat}{}^{-1}$)
r_d	rate of deactivation ($mmol\ min^{-1}\ g_{cat}{}^{-1}$)
r_{uc}	rate of uncatalyzed reaction ($mol\ min^{-1}\ cm^{-3}$)
R	universal gas constant ($kcal\ mol^{-1}\ K^{-1}$)
Re_p	particle Reynolds number
RMS	root mean square error
Sc	Schmidt number
Sh	Sherwood number
t	time – for continuous run (h), – for batch run (min)
T	temperature (K)
U	linear velocity than tubular section ($cm\ min^{-1}$)
U_{bed}	linear velocity in the bed ($cm\ min^{-1}$)
V_{abs}	volume of adsorbed liquid phase per gram of catalyst ($mL\ g_{cat}{}^{-1}$)
V_C	volume of single cell (mL)
V_L	liquid volume (mL)
V_R	volume of tubular reactor (mL)
V_{swell}	total swelling volume (mL)
V_{titr}	volume of titrating solution (mL)
W_{cat}	weight of catalyst (g)
x	conversion
z	axial coordinate (cm)

Greek letters

β	deactivation factor
η_{mix}	viscosity of the mixture ($g\ cm^{-1}\ min^{-1}$)
ν	stoichiometric coefficient
ρ	molar density ($mol\ cm^{-3}$)
ρ_{mix}	density of the mixture ($g\ mL^{-1}$)

Subscript

A	fatty acid
E	fatty acid methyl ester
h	height of bed
i	index for i-th component
j	index for j-th cell
M	methanol
n	index for n-th experimental data
T	triglycerides
W	water
0	reactor inlet

Superscript

B	bulk-external of resin
C	cell
calc	calculated value
exp	experimental data
R	internal of resin
ref	reference temperature (373.16 K)
S	surface of catalyst
uc	uncatalyzed reaction

the chemical regime but without the negative effect of breaking the catalyst particles as it occurs in well stirred reactors and with performances higher than the continuous tubular reactor, operating at high conversions, that works in diffusional regime.

In the present work, the esterification with methanol of a mixture of free fatty acids (oleins) has been studied in the presence of an acid exchange resin catalyst of the type Resindion Relite CFS in a pilot-size continuous fixed bed tubular reactor operated for relatively long time-on-stream. The experimental runs have been shown a progressive deactivation of the resin that we have observed mainly due to the presence of iron dissolved in the feeding mixture. The experimental data have been interpreted with a kinetic model based on an ionic-exchange reaction mechanism, reported in more details in our previous work [12], that takes into account also for the physical partitioning effects of the various components of the reacting mixture between internal and external liquid phase of the resin. The catalyst deactivation mechanism has been studied and we have found that the kinetics of the resin acid sites poisoning was essentially due to iron contained in the oleins mixture fed to the reactor. This aspect has been appropriately introduced in the dynamic reactor model to describe the experimental data.

In the final part of the work a study of the deactivation and regeneration of the Relite CFS resin is reported, in which batch esterification runs have been performed on a model mixture represented by soybean oil artificially acidified with oleic acid (about 50% by weight of oleic acid). These runs have been conducted on samples of resin taken at different axial positions in the tubular reactor at the end of the continuous run when the reactor was opened and the resin discharged. The aim of this set of runs was the study of the catalyst deactivation along the reactor axis and its influence on the reactor performances.

2. Experimental

2.1. Reactants and methods

The reactants used in the investigation are the following: methanol (Aldrich, purity > 99%, w/w), oleic acid (Carlo Erba, purity > 90%, w/w), and a commercially available acidity-free soybean oil (acidity < 0.3%, w/w). The oleins have been furnished by a local company (Parodi s.r.l.) and their composition in fatty acids is shown in Table 1. The amount of iron and other metals dissolved in this mixture has been analyzed by atomic absorption spectroscopy and the result are reported in Table 2.

The resin Relite CFS has been purchased by Resindion. This resin is a macroreticular copolymer styrene-DVB in wet form and their characteristics, as reported by the technical data sheet from the

Table 1
Fatty acids wt% composition of the oleins determined by GLC analysis.

Fatty acids	wt%
Caprylic acid, C8	0.16
Caprinic acid, C10	0.2
Lauric acid, C12	2.51
Myristic acid, C14	1.43
Palmitic acid, C16	31.3
Heptadecanoic acid, C17	0.1
Stearic acid, C18	3.49
Oleic acid, C18:1	43.46
Linoleic acid, C18:2	15.40
Linolenic acid, C18:3	1.22
Arachic acid, C20	0.29
Gadolenic acid, C20:1	0.20
Eicosadienoic acid, C20:2	0.05
Behenic acid, C22	0.08
Erucic acid, C22:1	0.06
Tricosanoic acid, C23	0.02
Average molecular weight	272.5 g/mol

Table 2
Metals content in the fatty acids mixture (oleins) (ppm).

Na	K	Ca	Cd	Cr	Fe	Mg	Mn	Zn
135	2.4	15.9	0.1	0.4	533	0.6	0.6	0.4

vendor, are summarized in Table 3. Before the experimental runs, resin has been dried, at 100 °C, for 24 h in a ventilated oven.

The withdrawn samples of the reaction mixture were analyzed by a standard acid–base titration procedure for the evaluation of the free residual acidity. The analysis repeatability has been improved by removing methanol in excess and water formed by heating in an oven prior to submitting the samples to titration.

A weighed amount of the sample was then dissolved in ethanol, some droplets of phenolphthalein as indicator were added, and the titration is then performed by means of an alkaline 0.1 M KOH solution. The volume of alkaline solution consumed is recorded, and the acidity of the sample can be calculated by means of the following relation:

$$\mathrm{Ac} = \frac{V_{\mathrm{titr}} C_{\mathrm{titr}} M_{\mathrm{OA}}}{1000 m_{\mathrm{sample}}} \times 100 \quad (\mathrm{wt\%}) \tag{1}$$

The acidity evaluated by Eq. (1) is referred to the oil phase (triglyceride + oleic acids + ester) with an error less than 1–2% on the free acidity expressed as weight percent of oleic acid.

The regeneration of the samples of exhaust resin, discharged from the reactor, has been made by contacting the resin with a mixture of sulfuric acid (50% by weight) for 24 h. After this treatment the resin was washed three or four times with demineralized water until washing solution reaches the neutrality. At the end of the washing procedure, the catalyst was dried in a ventilated oven for 24 h at 100 °C.

Table 3
Characteristics of the resins Relite CFS.

Matrix	Porous copolymer styrene-DVB
Functional groups	Sulfonics
Acidity	5.2 meq/g
Particles mean diameter	0.7 mm
Particles size range	0.3–1.18 mm
Total exchange capacity	1.7 eq/L
Maximum operating temperature	140 °C
Bulk density	0.325 g/cm^3

2.2. Continuous packed bed reactor

The scheme of the experimental apparatus, used for the continuous runs, is reported in Fig. 1. The reactor is composed by a stainless steel (AISI 304) tubular reactor with length 50 cm and an internal diameter of 8.2 cm. The catalytic bed contained 1 kg of exchange resin and 1.8 kg of stainless steel springs having the scope of compensating the swelling effect and avoiding an excessive pressure drop along the catalytic bed [17]. Methanol and fatty acids mixture (oleins) were mixed in a weight ratio 0.72:1 in a reservoir, gently mixed and preheated at 35 °C. This solution was fed to the reactor with a constant flow rate of 1 L/h. The reactor was kept at 100 °C and six bars in order to maintain methanol in a liquid state.

The reactor was operated continuously 11 h per day, for a total of 242 h, and samples were withdrawn at different times and at different heights of the reactor (respectively 0, 17, 33, 50 cm, see Fig. 1).

2.3. Batch reactor

The experimental apparatus used for the batch runs on the exhausted resin is described in details in our previous work [12]. The device is composed by a stainless steel tank reactor (volume 0.6 L) equipped with a magnetically driven stirrer and with pressure and liquid-phase temperature indicators. The reactor temperature is maintained at the prefixed value, within ±1 °C, by means of an electrical heating device connected to a PID controller. The reactor body is connected to a stainless steel pressurized chamber with a volume of 150 mL by means of which methanol can be added to the reaction system. The system is initially charged with the desired amount of acid oil and catalyst and, when the temperature reached the desired value, methanol is added using a nitrogen overpressure. This time instant represent the initial time for the reaction. During the run, small samples of liquid phase were withdrawn by using a line equipped with a stopping valve. In this way the evolution with time of the mixture acidity can be monitored for different reaction times.

3. Result and discussion

3.1. Experimental continuous runs

In the device reported in Fig. 1 a total of 23 continuous runs have been performed by feeding oleins mixture (acidity 95% by weight expressed as oleic acid) and methanol. The overall duration of this set of runs was of 242 h without changing the catalyst charged in the reactor. In each run, samples of the reacting mixture were taken at different positions (z-coordinate) along the reactor axis and in Table 4 the measured residual acidities are reported. From the data reported in Table 4, the loss in catalytic activity is evident, especially for the resin located in the first part (section between the inlet and z = 17 cm) and the intermediate part of the reactor (section between z = 17 cm and z = 35 cm).

From the values of acidity determined by titration, it is straightforward to evaluate the experimental conversion profile along the reactor by using the relation (2):

$$x_h^{\mathrm{exp}} = \frac{\mathrm{Ac}_0 - \mathrm{Ac}_h}{\mathrm{Ac}_0} \tag{2}$$

where Ac_0 is the acidity at the reactor inlet, while, Ac_h is the acidity determined at the height $z = h$. The activity loss of the catalyst can be expressed as in (3):

$$\mathrm{activity}_h = \frac{x_h^{\mathrm{exp}} - x_h^{\mathrm{uc}}}{x_h^{\mathrm{exp}}\big|_{t\to 0} - x_h^{\mathrm{uc}}} \tag{3}$$

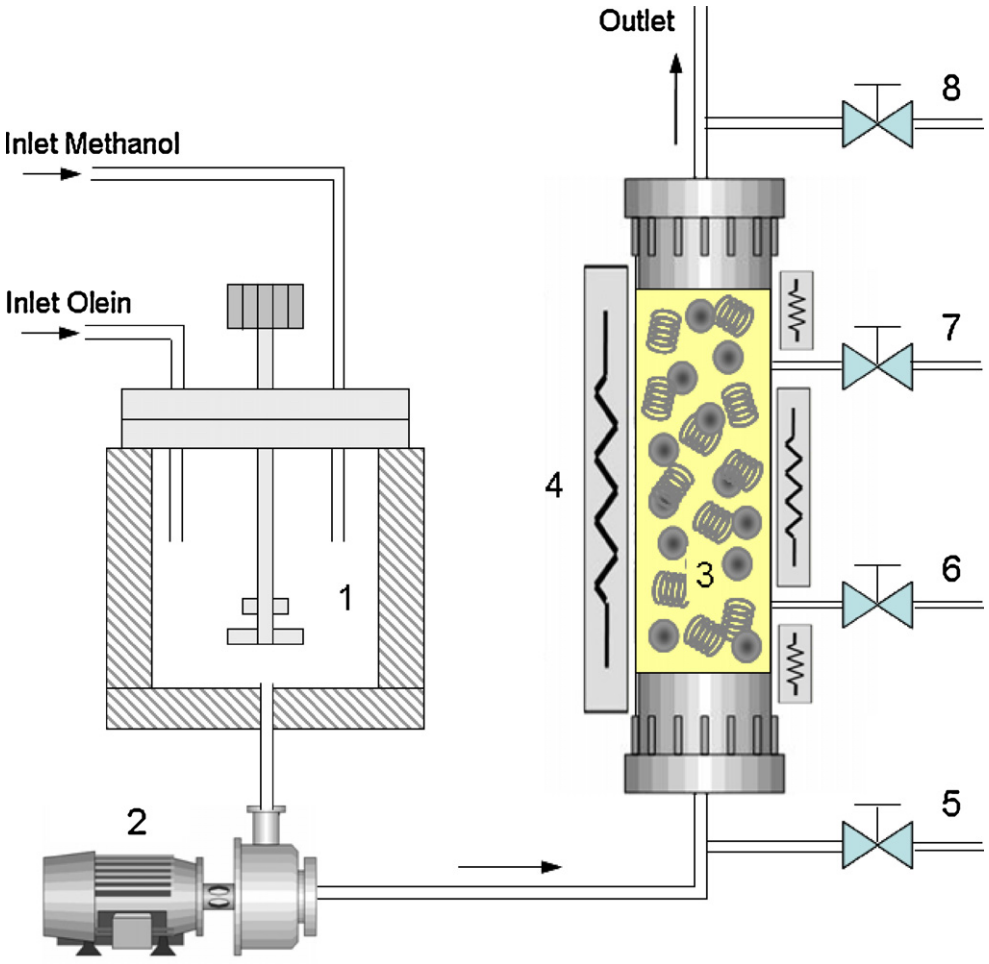

Fig. 1. Continuous reactor experimental apparatus. (1) Feeding reservoir containing free fatty acids and methanol; (2) feeding pump; (3) packed bed tubular reactor; (4) heating system; (5)–(8) valves for withdrawing samples of the reaction mixtures at different reactors heights (5, inlet; 6 and 7, intermediate heights; 8, outlet).

where x_h^{uc} is the conversion of the uncatalyzed reaction (estimated separately by a specific kinetic expression [14]), while, $x_h^{exp}\big|_{t\to 0}$ is the one of the catalyzed reaction in the absence of deactivation (corresponding to the initial time when the catalyst is assumed with full activity), both related to the different heights of the catalytic bed.

3.2. Kinetic model

3.2.1. (a) Uncatalyzed esterification

In a previous work, Tesser et al. [12] have described the kinetics of the uncatalyzed esterification reaction, with oleins as substrate, using a pseudo-homogeneous model by considering the reacting mixture as a single liquid phase and neglecting both the liquid–liquid eventual separation and the amount of volatiles compounds (mainly methanol and water) that are present in the head space of the reactor. The kinetic expression for the reaction rate is the following:

$$r_{uc} = kC_A^2C_M - k_{-1}C_AC_WC_E \simeq kC_A^2C_M \quad (4)$$

where C_A, C_M, C_W, and C_E are the liquid phase concentrations of, respectively, oleic acid or olein (A) methanol (M), water (W) and ester (E), k is the forward kinetic constant, k_{-1} is the reverse kinetic constant and r_{uc} is the reaction rate for the uncatalyzed reaction. The reaction kinetics was assumed of second order with respect to the acid concentration, as suggested by different authors [5,16,18], because this compound would act both as catalyst (in homogeneous phase) and reactant. In the derivation of the expression (4), the reverse term of the equilibrium reaction was neglected because the reactive system is always far from equilibrium conditions.

The Arrhenius equation, in a modified form, express the reaction rate constant as a function of temperature in the following way:

$$k = k^{ref}\exp\left[\frac{E_A}{R}\left(\frac{1}{T^{ref}} - \frac{1}{T}\right)\right] \quad (5)$$

In the expression (5), k^{ref} is the kinetic constant at a reference temperature T^{ref} chosen at 373.16 K, R is the universal gas constant and E_A is the activation energy. In Table 5 are reported the obtained kinetic parameters [12] related to the uncatalyzed esterification reaction for oleins mixtures.

3.2.2. Catalyzed esterification

Always in the previous work of Tesser et al. [12] a kinetic model has been developed, able to describe, with a sufficient accuracy, the esterification reactions of oleins catalyzed by Relite CFS in batch conditions, considering the real physico-chemical phenomenology that is the basis of the use of ionic exchange resins as catalysts: the phases partition phenomenon and the ionic exchange equilibrium.

3.3. Partition model

The partitioning phenomenon is of particular relevance when, as in this case, ionic exchange resins are used as catalysts in esterification reactions because water, produced by the reaction, is more selectively retained than methanol and other components and the

Table 4
Acidity wt% for experimental continuous runs at different times and at different heights of the reactor.

Run	Time (h)	Acidity% at 17 cm	Acidity% at 33 cm	Acidity% at 50 cm
1c	11	18.6	6.9	6.2
2c	14	18.5	8.6	9.6
	22	19.7	8.8	7.8
3c	28	19.3	8.2	7.3
	33	21.8	8.1	7.5
4c	40	21.8	8.9	7.2
	44	22.9	8.0	7.1
5c	51	22.6	8.1	6.9
	55	22.7	8.0	6.8
6c	62	25.8	8.7	7.3
	66	26.4	9.0	8.1
7c	73	28.7	9.1	7.3
8c	84	30.5	9.6	7.2
	88	35.3	9.7	8.1
9c	95	39.2	9.9	8.0
	99	39.9	9.8	8.2
10c	106	43.9	9.8	7.9
	110	42.8	9.4	7.8
11c	117	50.9	10.8	8.8
	121	52.3	11.3	9.4
12c	128	54.3	10.8	9.5
	132	57.6	11.8	9.2
13c	139	60.9	12.3	9.7
	143	62.0	13.2	10.4
14c	150	62.8	13.6	11.0
	154	67.2	14.0	11.7
15c	161	63.9	14.6	11.4
	165	63.1	13.6	10.6
16c	172	66.1	17.1	12.9
	176	66.9	17.1	13.4
17c	183	67.5	20.6	13.9
	187	70.6	20.2	13.8
18c	194	73.3	21.8	14.3
	198	74.9	23.7	15.3
19c	209	72.5	27.2	19.5
20c	220	73.9	35.2	19.9
21c	227	73.5	32.8	19.8
22c	234	75.7	37.6	20.0
23c	242	77.3	39.1	23.7

composition inside the particles (that is crucial for the reaction) is very different from that of bulk liquid phase. Another important aspect is that this phenomenon cannot be neglected when a great amount of exchange resin is used, because, the amount of absorbed water, in this case, is significantly high. Water and methanol absorbed interacts with both fixed anionic groups ($-SO_3^-$), and relatively mobile protonated molecules (methanol or water) forming a primary solvation shell containing 4–6 molecules [19]. Other molecules can then further aggregate to form clusters of methanol and/or water [19] that are responsible of the swelling effect. Initially, we have only clusters surrounding protonated methanol. Entering water molecules displace methanol that goes outside the particle and new mixed clusters are formed. A volume based Langmuir expression [12] can easily be derived considering as driving force the volume filling degree. According to this model, for a multicomponent mixture, following Eq. (6) can be used for relating the external (superscript B, bulk) to the internal (superscript R, resin) concentration for each of the partitioned components in equilibrium condition:

$$C_i^R = \frac{K_i^{eff} C_i^B}{\sum_n K_n C_n^B} \text{ with } i \text{ or } n = \text{A (oleic acid or olein), M (methanol), E (methyl ester), W (water)} \quad (6)$$

where C_i^R and C_i^B are the concentration of the i-th component in the bulk phase and inside the resin respectively, K_j is the partition constant, while, K_i^{eff} represent the effective partition constant that takes into account for the molecular size of the pure i-th component through the introduction of its molar density ρ_i and molecular weight M_i through the relation (7).

$$K_i^{eff} = \frac{K_i \rho_i}{M_i} \quad (7)$$

In our specific system, the physical equilibrium for eventual triglycerides partition has been neglected due to their relatively high molecular size. All the parameters related to the partitioning model used in the present work, are reported in Table 6 and have been experimentally evaluated [12], for the resin Relite CFS, at a temperature of 100 °C. More details about these data can be found in the mentioned paper [12]. Moreover, the partition parameters related to the binary system water/methanol have been experimentally determined, while the same parameters related to the other binaries in the absence of experimental data have approximately estimated, on the basis of the following considerations. For what concerns the fatty acids and their corresponding methylesters, we have assumed that the differences in polarity and molecular sizes among them are almost the same of those between water and methanol. In such a way, as a rough approximation, the partition constant for the fatty acid is assumed equal to that of water ($K_A = K_W$), while the constant for methylester is assumed equal to that of methanol ($K_E = K_M$). With these assumptions, the effective partition constants determine the competitive adsorption of the various components in the quaternary system considered (methanol, water, methylester and fatty acid) according to their molecular weight (molecular size) and polarity.

Table 6
Partition constants [12].

Component	K_i (mL mol^{-1})	K_i^{eff}
Water	1	0.0542
Methanol	0.317	0.0069
Fatty acid in olein	1	0.0030
Ester	0.317	0.00088

3.4. Reaction mechanism

A reliable reaction mechanism has been proposed and discussed in a previous work [12] such as in the following scheme:

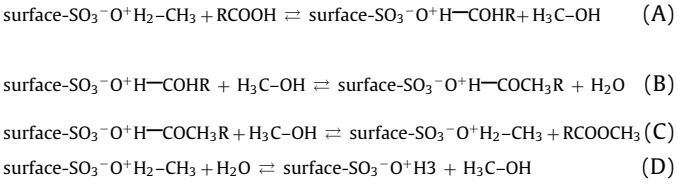

Table 5
Kinetic and ion-exchange parameters [12].

Uncatalyzed reaction	Catalyzed reaction	
$k_{uc}^{ref} = 65.78$ mL^2 mol^{-2} min^{-1} $E_{A,uc} = 16.28$ kcal mol^{-1}	$k_{cat}^{ref} = 13.07$ mL $g_{cat^{-1}}$ min^{-1} $E_{A,cat} = 12.77$ kcal mol^{-1} $k_{-cat}^{ref} = 3.85$ mL $g_{cat^{-1}}$ min^{-1} $E_{A,-cat} = 7.96$ kcal mol^{-1}	$H_A = 0.31$ $H_W = 1.55$ $H_E = 0.17$

By assuming that the step B, an Eley–Rideal reactive event, is rate determining step (RDS) the following expression can be derived for the overall reaction rate [12]:

$$r_{cat} = \frac{k_{cat}H_A C_A^R - k_{-cat}(H_E C_E^R C_W^R / C_M^R)}{1 + (H_A C_A^R / C_M^R) + (H_E C_E^R / C_M^R) + (H_W C_W^R / C_M^R)} \quad (8)$$

In relation (8) k_{cat} and k_{-cat} are the kinetic constants for, respectively, the forward and the reverse catalyzed reaction that are both functions of temperature according to the Arrhenius relation (Eq. (5)); H_A, H_W and H_E are the ionic exchange equilibrium constants for the reactions of protonated methanol with, respectively, fatty acid, water and methylester and we have assumed that the constants are independent from temperature; C_i^R is the concentration of the various components in the resin-absorbed liquid phase. The kinetic and equilibrium exchange parameters are summarized in Table 5. The detailed procedure for the derivation of Eq. (8) is reported in reference [12] and the presence of the equilibrium dimensionless parameters H is the consequence of the mathematical derivation of the reaction rate expression from the assumed sequence of elementary steps.

3.5. Packed bed reactor (PBR) model in stationary state and without catalyst deactivation

The low flow rates used in the continuous experimental runs, determine the existence of diffusional resistance to the external mass transfer at the interface fluid-particle [15]. In order to quantitatively evaluate the extension of this phenomenon a first mathematical model has been developed that is able to describe the stationary behavior of the PBR reactor, in absence of catalyst deactivation phenomena, by considering as the unique experimental data the acidity profile along reactor axis after the first 11 h run (run no.1 in Table 4).

For this model, the mass balance along the reactor axis (z-coordinate) is described by the following system of ordinary differential Eq. (9):

$$\frac{dC_i^B}{dz} = \nu_i \frac{1}{U} r_{cat} C_{cat} + \nu_i \frac{1}{U}\left(r_{uc}^R \frac{V_{swell}}{V_R} + r_{uc}^B \varepsilon\right) \quad (9)$$

where ν_i is the stoichiometric coefficient (−1 for A and M, +1 for E and W), U is the linear fluid velocity evaluated on the full geometrical cross section of the tubular reactor, C_{cat} is the catalyst concentration calculated as mass of catalyst per reactor volume V_R, ε is the void fraction assumed equal to 0.23, V_{swell} is the total volume of liquid absorbed by the resin ($V_{swell} = V_{abs} \times$ weight of catalyst, where V_{abs} is the specific swelling volume of the resin in the presence of only methanol, experimentally evaluates as 0.790 mL g_{cat}^{-1}), r_{cat} is the catalyzed reaction rate described by relation (8) while r_{uc}^R and r_{uc}^B are the uncatalyzed reaction rates in the absorbed and bulk phases respectively, both expressed according to the relation (4) in which are introduced the corresponding concentration of the resin-absorbed phase and the bulk liquid phase.

The mass transfer resistance has been described, according to the theory of boundary layer, by considering that a concentration gradient between the bulk liquid and the catalyst surface is present. In this way, is the surface concentration that intervenes in the partitioning phenomenon between the external and internal (absorbed) liquid phase and in the equation (6) appears the surface concentration C_i^S instead that of bulk C_i^B. Assuming that a pseudo-steady state holds for the mass transport, the amount of each reactant consumed by the reaction must be equal to the amount transferred by diffusion from bulk to the catalyst surface. This concept is expressed mathematically by the relation (10).

$$k_S a_S (C_i^B - C_i^S) = -\nu_i r_{cat} C_{cat} - \nu_i r_{uc}^R \frac{V_{swell}}{V_R} \quad (10)$$

where k_S is the mass transfer coefficient, a_S is the specific interface area (cm^2 cm^{-3}), estimated as the external geometric surface area of the resin per unit of reactor volume and assuming that the swollen resin particle are like rigid spheres. The estimation of k_S can be done both from literature correlation or, alternatively, from regression analysis of the experimental data considering this mass transfer coefficient as an adjustable parameter. In the present work, the correlation proposed by Olive (see Seguin et al. [20]), represented by the following expression:

$$Sh = 4.4 Re_p^{0.35} Sc^{(1/4)} = \frac{k_s d_p}{D_{eff}} \quad [0.004 < Re_p < 1.78] \quad (11)$$

has been used. From this relation the value of mass transfer coefficient can also be evaluated and introduced in the Eq. (10).

The particle Reynolds number is calculated by the following expression

$$Re_p = \frac{d_p U_{bed} \rho_{mix}}{\eta_{mix}} \quad (12)$$

where d_p is mean diameter of the resin particle (0.08 cm), this represent an approximate estimation of the swollen particles diameter (particles are not uniform in size) in the interior of the catalytic bed where the presence of the metallic springs limit the swelling phenomenon. This value for the averaged particle diameter has been used for the calculation of the Reynolds number), D_{eff} is the effective diffusivity, U^B is linear velocity of mixture through the bed, ρ_{mix} and η_{mix} are density and viscosity of mixture. The particle Reynolds number in which this correlation was developed is compatible with our experimental runs ($Re_p = 0.5$) and the correlation should furnish a suitable mean estimation of k_S equal 0.210 cm min^{-1}.

In our calculations this parameter was referred to the diffusion of oleic acid and was assumed, as a first approximation, the same for all the components. In the application of Eq. (11) to the estimation of mass transfer coefficient, pure components properties depending on temperature and composition like viscosity and density have been evaluated by using the databank of a commercial process simulator (Chemcad 5.2). The properties of the mixture have been evaluated according to Reid et al. [21] for what concerns viscosity and density while the diffusivity has been calculated as reported by Santacesaria et al. [15]. It is therefore possible to express the experimental result in terms of residual wt% acidity as oleic acid with respect to the weight of non-volatiles compounds (acid, ester and triglyceride) according to Eq. (13):

$$Ac^{calc} = \frac{C_A^B M_A}{C_A^B M_A + C_E^B M_E + C_T^B M_T} \times 100 \quad (13)$$

In Fig. 2 is reported the acidity profile calculated according to the expression (13) in comparison with the experimental data collected. From this plot a good agreement between the data and the developed model can be appreciated.

3.6. Deactivation

The poisoning effect observed on the resin could be attributed to both fouling phenomena derived from the raw nature of the feed and to ionic exchange with metals, also present in the feed, that deactivate the catalytic acid sites of the resin. This last effect can be considered predominant being the feed relatively rich in iron as can be appreciated in Table 2. Although sodium would contribute to catalyst deactivation, we observed a negligible effect of this metal even if it is present in a relatively high concentration, as reported in Table 2. This was confirmed by the experimental observation that sodium was not accumulated in the resin particles, probably because iron and other metals like chromium are more selectively retained. As a further visual confirmation of the resin poisoning and alteration with respect to its initial state, in Fig. 3 some photographs

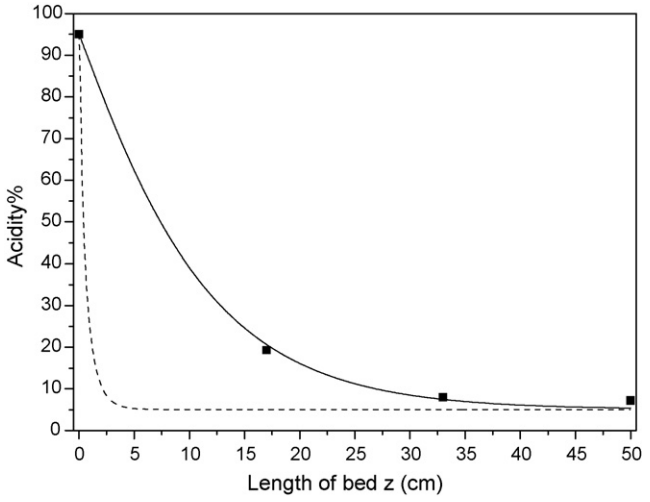

Fig. 2. Acidity profile along the catalytic bed in the absence of deactivation phenomena. (■) Experimental data (run 1); (—) simulation in diffusive regime; (- - -) simulation in kinetic regime.

are reported that show the resin discharged from the various sections of the reactor at the end of the sequence of continuous runs. A pronounced difference in color is evident between the samples of resin located at different positions along the reactor longitudinal axis being darker the resin located near the reactor inlet. The darker color of the resin seem to be related with its more pronounced deactivation as will be shown later from the samples taken at 17 cm from the inlet that are characterized by the more evident deactivation with time.

3.7. Packed bed reactor (PBR) model in transient condition in the presence of deactivation

In this work, a mathematical model able to simulate the dynamic behavior of the packed bed tubular reactor has been developed. This model considers the tubular reactor approximated by a sequence of 50 different cells operating as dynamic CSTRs in series. This model consider also the physical partition of the reagents and products between the internal and the external part of the catalytic particles, the chemical absorption on the catalytic sites and the effect of the external mass transfer. The mass balance of the j-th cell is given by the following system of differential equations:

$$V_L^C \frac{dC_{i,j}^B}{dt} = \left[QC_{i,j-1}^B - QC_{i,j}^B + \nu_i \left(r_{uc,j}^B V_L^C + r_{uc,j}^R V_{swell}^C + r_{cat,j} W_{cat}^C \right) \right] \times 60 \quad (14)$$

where Q is the volumetric flow rate of oil and methanol, $C_{i,j}^B$ is the concentration of the i-th component in the liquid bulk of the j-th cell. The superscript C, that appears in the Eq. (14), means that the related value corresponds to a single cell, therefore, V_L^C, V_{swell}^C, W_{cat}^C are respectively the bulk liquid volume, the swelling volume of the resin and the mass of the catalyst all referred to a single reaction cell. Moreover, $r_{uc,j}^B$ ed $r_{uc,j}^R$ are the uncatalyzed reaction rates, respectively in the liquid bulk and in the resin of the j-th cell. These reaction rates are calculated with the following relations (15) and (16):

$$r_{uc,j}^B = k\left(C_{A,j}^B\right)^2 C_{M,j}^B \quad (15)$$

$$r_{uc,j}^R = k\left(C_{A,j}^R\right)^2 C_{M,j}^R \quad (16)$$

$r_{cat,j}$ is the catalyzed reaction rate that can be calculated with relation (17):

$$r_{cat,j} = \frac{\beta_j (k_{cat} H_A C_{A,j}^R - k_{-cat}(H_E C_{E,j}^R C_{W,j}^R / C_{M,j}^R))}{1 + (H_A C_{A,j}^R / C_{M,j}^R) + (H_E C_{E,j}^R / C_{M,j}^R) + (H_W C_{W,j}^R / C_{M,j}^R)} \quad (17)$$

In the relation (17), β_j is a deactivation parameter, variable from 0 to 1 that depends on the specific catalyst poisoning mechanism and the corresponding kinetics.

The mass transfer limitation has been evaluated by assuming a pseudo-steady state condition for the amount of fatty acid diffusing and reacting. According to this condition we can write:

$$k_S a_S \left(C_{i,j}^B - C_{i,j}^S\right) = -\nu_i \left(r_{cat,j} C_{cat} + r_{uc,j}^R \frac{V_{swell}^C}{V_C} \right) \quad (18)$$

where $C_{i,j}^S$ is the concentration of the i-th component on the surface of the resin in the j-th cell and V^C is the volume of a single cell.

The concentrations of each component in the liquid bulk and on the surface of the resin are related through the partitioning equilibrium and can be calculated by relations (19).

$$C_{i,j}^R = \frac{K_i C_{i,j}^S \rho_i / M_i}{\sum_n K_n C_{n,j}^S} \quad (19)$$

3.8. Kinetics of catalyst deactivation

The catalyst deactivation parameter β_j, as said before, depends on the mechanism of catalyst poisoning and the corresponding kinetics. By analyzing the poisoned catalyst for the iron content, it has been observed that poisoned resin retains large amounts of iron that is present in the fatty acids mixture fed to the reactor. For this reason we have attributed to the presence of iron the main effect of catalyst deactivation. The effect of poisoning can then be interpreted as the result of a reaction of the type:

$$Fe^{q+} + \alpha site_{free} \xrightarrow{k_d} \alpha site_{occupied} \quad (20)$$

a power law kinetics of the type expressed by relation (21) can be assumed valid, as a first approximation, for the description of catalytic site poisoning:

$$r_d = k_d C_{Fe} (C_\sigma)^\gamma \quad (21)$$

where, r_d is the rate of poisoning (mmol min^{-1} g$_{cat}^{-1}$), k_d is the deactivation constant, C_{Fe} is the iron concentration in the feed (mmol mL^{-1}), C_σ is the concentration of active sites per gram of resin (meqH$^+$ g$_{cat}^{-1}$), α is the mole number of active sites poisoned per mole of adsorbed iron and γ is the exponent that identify the reaction order with respect to active sites concentration. The best value for α resulted equal to 3, while, a value of 2, for γ, was estimated. The first order with respect to iron concentration (see Eq. (20)) has furnished the lowest mean square error between experimental and calculated values (best fitting).

Deactivation kinetics is taken into account in the previously described dynamic model of the tubular reactor by considering the mass balance related to the poison (Fe) in each cell, as reported in the following differential equation:

$$V_L^C \frac{dC_{Fe,j}}{dt} = (Q\, C_{Fe,j-1} - Q\, C_{Fe,j} - r_{d,j}\, W_{cat}^C) \times 60 \quad (22)$$

where the rate of poison disappearing from the liquid bulk, $r_{d,j}$, is given by:

$$r_{d,j} = k_d C_{Fe,j} \left(C_\sigma^0 \beta_j\right)^\gamma \quad (23)$$

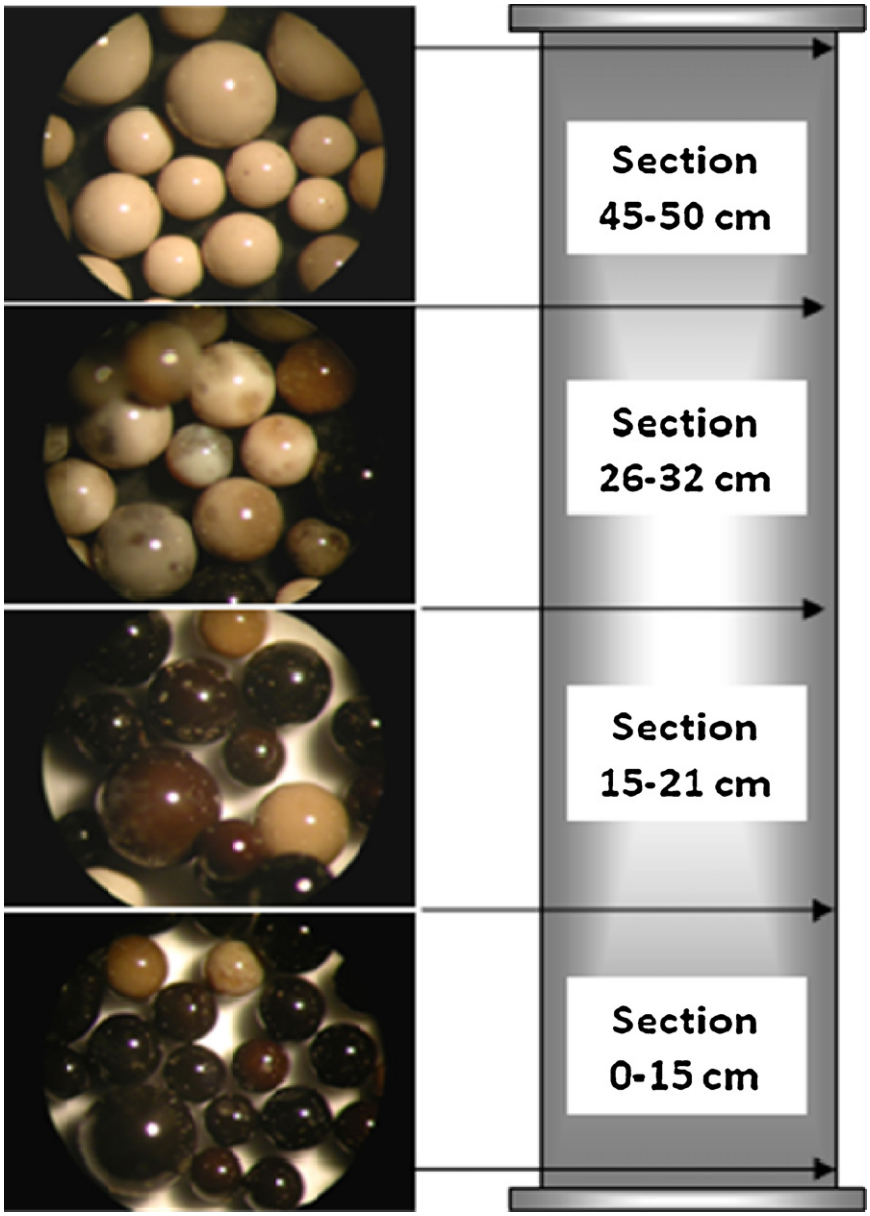

Fig. 3. Microphotographs of resin particles discharged from various section of the reactor after the sequence of continuous runs.

In this relation C_σ^0 is the initial concentration of the acid sites of the resin. The deactivation factor β_j corresponds to the ratio between the un-poisoned residual and the initial acid sites for each cell. In order to evaluate β_j, the mass balance on the un-poisoned acid sites, represented by relation (24), must be solved.

$$\frac{d\beta_j}{dt} = -\alpha \frac{r_{d,j}}{C_\sigma^0} \times 60 \tag{24}$$

The initial conditions for solving the deactivation model are:

$$C_{Fe,j}(t=0) = 0.00450\,\text{mmol mL}^{-1} \tag{25}$$

$$\beta_j(t=0) = 1$$

The described dynamic model of the tubular reactor with deactivation can be solved by a numerical approach, using the Rosenbrock algorithm for the solution of the ordinary differential equation system. In the meantime the only adjustable parameter, k_d, has been determined by applying nonlinear fitting that minimizes the following objective function represented by a quadratic mean square error between the experimental and calculated acidities.

$$\text{RMS} = \sqrt{\frac{1}{N}\sum_{n=1}^{N}\left(\text{Ac}_{h,n}^{\text{exp}} - \text{Ac}_{j=h,n}^{\text{calc}}\right)^2} \tag{26}$$

The acidity profiles for different reactor heights have been calculated by Eq. (27)

$$\text{Ac}_j^{\text{calc}} = \frac{C_{A,j}^B M_A}{C_{A,j}^B M_A + C_{E,j}^B M_E + C_{T,j}^B M_T} \times 100 \tag{27}$$

In Fig. 4 are reported both experimental data in terms of activity$_h$ and the results of a simulations by assuming a deactivation constant k_d equal to 0.221 g_{cat} mL min^{-1} meq$H^{+\,-2}$. By observing Fig. 4 it is possible to appreciate the good agreement obtained for the profiles related to the intermediate sections located at z = 17 and 33 cm.

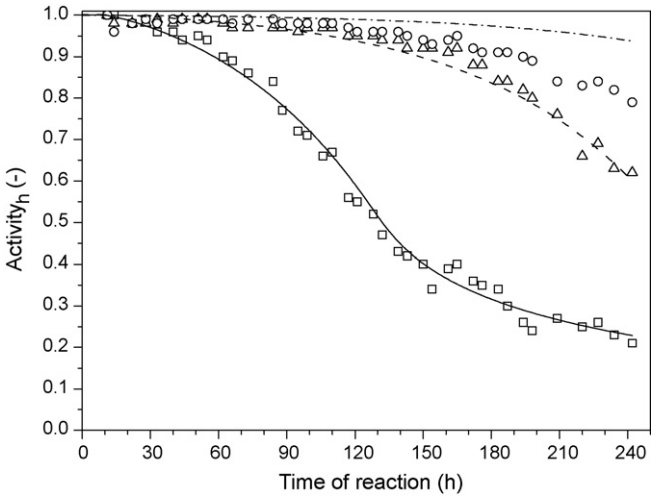

Fig. 4. Continuous runs in pilot-scale packed bed reactor. Loss in catalytic activity for various reactor sections during the operation. (□) Experimental data at 17 cm; (△) experimental data at 33 cm; (○) experimental data at reactor outlet (50 cm); (—) simulation at 17 cm. (- - -) simulation at 33 cm; (– · –) simulation at reactor outlet.

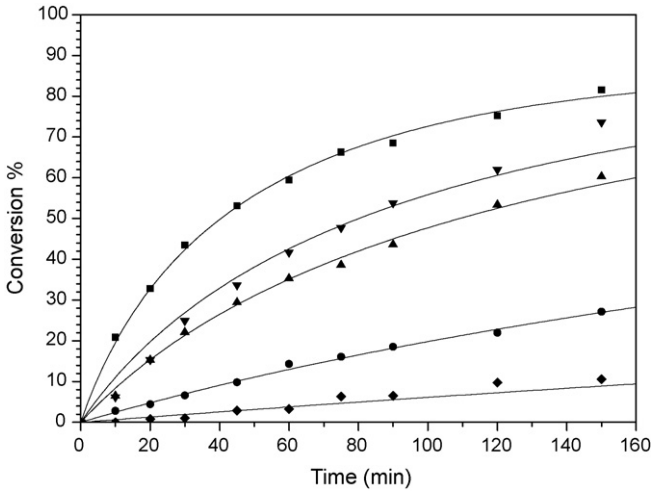

Fig. 5. Result of batch runs on soybean oil–oleic acid mixture (50/50, w/w) at 100 °C and 1 g of catalyst. (■) Fresh resin; (▼) averaged resin sample of section 33–50 cm; (▲) averaged resin sample of 17–33 cm; (●) Averaged resin sample of section 0–17 cm; (♦) uncatalyzed esterification; (—) model simulation.

On the contrary, the experimental profile at the reactor outlet is not adequately simulated. This is probably due to the additional release of chromium ions from the stainless steel springs used as catalyst diluent. In this hypothesis chromium acts as further poison for the catalyst and its detrimental effect results particularly evident in the last part of the reactor, near the outlet section. This phenomenon, although experimentally observed by measuring chromium concentration in the outlet stream, has not been included in the developed model because it was dependent on the particular device employed. However, by assuming that a single chromium atom deactivates a single active site (1:1 stoichiometry), the loss in activity of the resin due to chromium can be approximately estimated to be about 6.2%. The value of 6.2% of activity loss, has been estimated as follows: the final chromium concentration in the resin is 1.68% corresponding to 0.32 meq Cr/g resin. Considering a 1:1 stoichiometry, we obtain 0.32 meq of active sites poisoned per gram of resin. By taking into account that the initial active sites concentration in the resin is of 5.2 meq/g, the loss of activity is therefore of 6.2%. The difference between the calculated final activity (see Fig. 4) and the experimental value at 50 cm (exit of the reactor) is about 13%. A similar activity loss can therefore be explained with an average stoichiometry of 1:2 (one chromium atom poison two active sites) that is quite reasonable.

The experimental evidences of the exposed consideration are represented by XRF (X-ray fluorescence) analysis reported in Table 7 performed on each portion of the resin discharged from different reactor sections. As it can be seen, iron is adsorbed mainly in the first part of the reactor while chromium concentration increases along the catalytic bed. From further analyses conducted by AAS (atomic absorption spectroscopy) after the last run (run 23, 242 h on stream) on the bulk liquid phase, a maximum in chromium concentration has been detected approximately in the middle of the catalytic bed, in the section at $z = 33$ cm and this represent an indication that the chromium ion are released by the metallic spring of the previous section and accumulate here while, in the final part of the catalytic bed, the chromium content in the liquid resulted reduced of about 50%, an indication that this metal was adsorbed by resin located in the last reactor section. The observed chromium release is very probably due to the relatively high acidity of the feed (around 95% by weight of oleic acid) and to the relatively long duration of the tests.

3.9. Modeling of experimental batch runs

The catalytic resin discharged from the reactor has then been submitted to an activity test conducted in batch conditions. A total of seven runs have been performed by using 1 g of resin, 100 g of refined soybean oil and 100 g of oleic acid. In this way a 50% by weight acidic substrate, free from poisoning agents, has been obtained. For the batch runs, enough methanol was added in order to have a molar ratio methanol/oleic acid of 8:1. The reaction mixture was stirred at 1500 rpm and maintained at 100 °C for the whole reaction time (150 min). During the reaction, nine samples of liquid phase were withdrawn from the reactor and were used for acidity determination as previously described. In Fig. 5 the comparison is reported, in terms of percent conversion, between the performances obtained with, respectively, fresh and poisoned resin used as samples averaged on the three following reactor sections: 0–17, 17–33 and 33–50 cm.

In the development of this batch reactor model, we have made the assumption that the system is always in physical equilibrium in a way that the concentration of the reactants and products inside the resin can be evaluated from the corresponding bulk concentrations according to the Eq. (6). The evolution with time of the moles of each component can be evaluated by solving the following material balance based on a set of ordinary differential equation (ODE) expressed by the relation (28):

$$\frac{dn_i}{dt} = \nu_i(r_{uc}^{B}\, V_L + r_{cat}\, W_{cat}) \tag{28}$$

where n_i represent the overall mole number of the i-th specie and W_{cat} is the weight of catalyst loaded in the reactor. At each integration step in time of the system (28) the partitioning equilibrium must be solved by imposing the congruence balance Eq. (29):

$$n_i^{R} + n_i^{B} = n_i \tag{29}$$

where n_i^{R} and n_i^{B} are, respectively, the moles of i-th component in the resin and in the bulk. The number of moles n_i^{R} are obtained as simultaneous solution of the set of nonlinear algebraic Eq. (6) and the explicit algebraic Eq. (30):

$$n_i^{R} = C_i^{R}\, V_{swell} \tag{30}$$

The moles in the bulk phase, n_i^{B}, are calculated from Eq. (29) while the bulk concentration are evaluated from the following rela-

Table 7
Analysis of iron and chromium poisons after 242 h of reaction.

	Resin phase: XRF analysis				Bulk phase: AAS analysis		
	Fresh (wt%)	0–15 cm[a] (wt%)	27–33 cm[a] (wt%)	45–50 cm[a] (wt%)	17 cm[b] (ppm)	33 cm[b] (ppm)	50 cm[b] (ppm)
Cr	–	0.16	1.18	1.68	0.4	23.4	10.4
Fe	0.089	49.51	24.39	8.44	197	27.0	6.5

[a] Analysis on the resin discharged.
[b] Analysis of liquid phase sampled.

tion (31):

$$C_i^B = \frac{n_i^B}{V_L} \tag{31}$$

The experimental run with fresh catalyst has been simulated by adjusting the parameters k_{cat} and k_{-cat} (Table 8), being the kinetic constants reported in Table 5 related to the use of a complex mixture of fatty acids (oleins). For the uncatalyzed reaction the kinetic constant k, from Tesser et al. [12], has been used. For the experimental batch runs performed on deactivated and regenerated catalyst, the deactivation parameter β has been adjusted by regression on the experimental data and the kinetic expression adopted is represented by relation (32) that is formally identical to Eq. (17) in which the cell subscript has been dropped.

$$r_{cat,j} = \frac{\beta_j(k_{cat}H_A C^R_{A,j} - k_{-cat}(H_E C^R_{E,j} C^R_{W,j}/C^R_{M,j}))}{1 + (H_A C^R_{A,j}/C^R_{M,j}) + (H_E C^R_{E,j}/C^R_{M,j}) + (H_W C^R_{W,j}/C^R_{M,j})} \tag{32}$$

All the experimental results and the parameters used for the simulations of the batch runs like the ones reported in Fig. 5 are reported in Table 8. The kinetic parameters related to the catalyzed esterification are different from those reported in Table 5, because, they are related to an artificial mixture soybean oil/oleic acid rather than to a mixture of fatty acids (olein). In Fig. 5, a comparison is reported between experimental and simulated conversion/time profiles for both fresh and deactivated resin. It is interesting to observe that, as it can be expected, the catalytic activity corresponding to the resin from different reactor sections is related to the deactivation extent along the position as illustrated previously for continuous runs on oleins feedstock. As a matter of fact, the averaged sample of the section 0–17 cm seems to be almost completely deactivated and shows a residual activity in esterification of oleic acid that is less than 10% if compared to that of the fresh catalyst for the same reaction (the value of 10% has been estimated by considering the fresh catalyst correspondent to 100% of activity and the uncatalyzed reaction as 0%). The subsequent sections of the catalytic bed, 17–33 and 33–50 cm, respectively, resulted less deactivated at the end of the series of continuous runs and are characterized by a residual activity of, respectively, 35% and 48%.

In Fig. 6 a comparison is reported between experimental and simulated conversion/time profiles for fresh and regenerated catalyst. An almost complete regeneration has been observed for the catalyst taken from the first 0 to 17 cm section while the catalyst from the subsequent sections has recovered its activity only partially up to a level of about 75%. This difference in activity recovery has been attributed to the presence of a relatively high chromium concentration adsorbed on these portions of catalyst. Chromium ions resulted more difficult to remove, with the adopted regeneration procedure, with respect to iron. On the contrary, iron, being continuously introduced in the system together with the reactant, shows a poisoning effect that is mainly concentrated on the first part of the reactor.

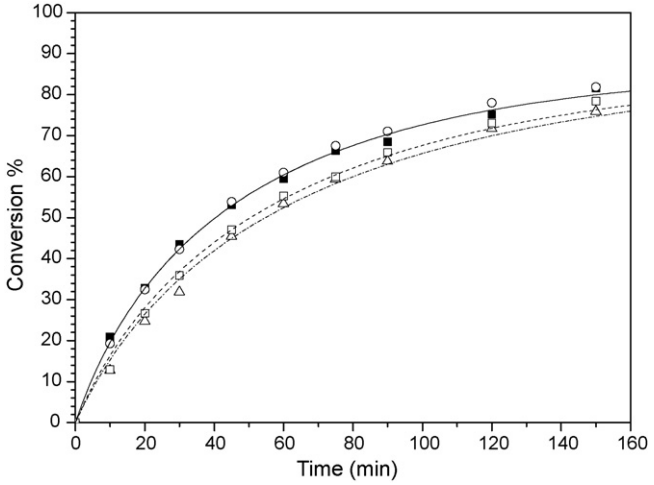

Fig. 6. Result of batch runs on soybean oil–oleic acid mixture (50/50 by wt) at 100 °C and 1 g of catalyst. Effect of resin regeneration. Comparison between fresh, deactivated and regenerated catalyst. (■) Fresh resin; (○) regenerated sample of section 0–17 cm; (△) regenerated sample of section 17–33 cm; (□) regenerated sample of section 33–50 cm. Continuous and dashed lines are related to the corresponding model simulations.

4. Conclusions

This study has shown that the deactivation phenomenon of ionic exchange resins, frequently used as catalysts in the esterification of fatty acids mixtures, is mainly due to the ionic exchange of the proton with iron or other metals that can be present in the feedstock probably as a consequence of the corrosive action of free fatty acids during their storage in tanks. A dynamic model has been developed for describing the performances of a pilot-scale continuous tubular reactors containing exchange resins, more or less diluted with an inert material. The model can be usefully used to approximately forecast the lifetime of the catalyst if the amount of iron dissolved in the feedstock is known. By taking into account that, very frequently, oleins and other acid substrates are stored in iron container, in this

Table 8
Result for batch runs on acidified soybean oil (50 wt%).

Run	Resin	Parameter
1b	Fresh resin	$\beta = 1.00$
2b	Deactivated (section 0–17 cm)	$\beta = 0.07$
3b	Deactivated (section 17–33 cm)	$\beta = 0.35$
4b	Deactivated (section 33–50 cm)	$\beta = 0.48$
5b	Regenerated (section 0–17 cm)	$\beta = 1.00$
6b	Regenerated (section 17–33 cm)	$\beta = 0.72$
7b	Regenerated (section 33–50 cm)	$\beta = 0.77$

work, relevant information has also been obtained concerning the selection of a suitable material in contact with the acid fluid and feedstock storage modality in order to maximize the catalyst lifetime by minimizing the poisoning effect due to the presence of metal ions.

In the paper, it has also been shown that the acid exchange resin can be regenerated. At last, it is very important to point out that this work has shown the relevance of the selectivity in water absorption that cannot be neglected when the amount of resin used is high as it occurs in pilot and industrial packed bed reactors.

Acknowledgments

Thanks are due to ASER srl Co. and to MAE (Italian Ministry of Foreign Affairs – Ministero degli Affari Esteri) for funding the research.

References

[1] F.R. Ma, M.A. Hanna, Biodiesel production: a review, Biores. Technol. 70 (1999) 1–15.
[2] H. Fukuda, A. Kondo, H. Noda, Biodiesel fuel production by transesterification of oils, J. Biosci. Bioeng. 92 (2001) 405–416.
[3] H. Van Gerpen Jon, Biological and Agricultural Engineering, University of Idaho, Moscow, ID, USA. www.deq.state.mt.us. (Biodiesel Economics, Montana Economics 2007).
[4] D. Kusdiana, S. Saka, Kinetics of transesterification in rapeseed oil to biodiesel fuel as treated in supercritical methanol, Fuel 80 (2001) 693–698.
[5] C. Lacaze-Dufaure, Z. Mouloungui, Catalysed or uncatalysed esterification reaction of oleic acid with 2-ethyl hexanol, Appl. Catal. A: Gen. 204 (2000) 223–227.
[6] M. Berrios, J. Siles, M.A. Martìn, A. Martìn, A kinetic study of the esterification of free fatty acids (FFA) in sunflower oil, Fuel 86 (2007) 2383–2388.
[7] S. Pasias, N. Barakos, C. Alexopoulos, N. Papayannakos, Heterogeneously catalyzed esterification of FFAs in vegetable oils, Chem. Eng. Technol. 29 (11) (2006) 1365–1371.
[8] S.D. Alexandratos, Ion exchange resins: a retrospective from industrial and engineering chemistry research, Ind. Eng. Chem. Res. 48 (2009) 388–398.
[9] F.G. Helferrich, Ion Exchange, Dover Science Books, 1995 (Chapter 5).
[10] T. Popken, L. Gotze, J. Gmehling, Reaction kinetics and chemical equilibrium of homogeneously and heterogeneously catalyzed acetic acid esterification with methanol and methyl acetate hydrolysis, Ind. Eng. Chem. Res. 39 (2000) 2601–2611.
[11] W. Song, G. Venimadhavan, J.M. Manning, M.F. Malone, M.F. Doherty, Measurement of residue curve maps and heterogeneous kinetics in methyl acetate synthesis, Ind. Eng. Chem. Res. 37 (1998) 1917–1928.
[12] R. Tesser, L. Casale, D. Verde, M. Di Serio, E. Santacesaria, Kinetics and modeling of fatty acids esterification on acid exchange resins, Chem. Eng. J., in press, doi:10.1016/j.cej.2009.12.050.
[13] R. Tesser, M. Di Serio, M. Guida, M. Nastasi, E. Santacesaria, Kinetics of oleic acid esterification with methanol in the presence of triglycerides, Ind. Eng. Chem. Res. 44 (2005) 7978–7982.
[14] E. Santacesaria, R. Tesser, M. Di Serio, M. Guida, D. Gaetano, A. Garcia Agreda, Kinetics and mass transfer of free fatty acids esterification with methanol in tubular packed bed reactor: a key pre-treatment in biodiesel production, Ind. Eng. Chem. Res. 46 (15) (2007) 5113–5121.
[15] E. Santacesaria, R. Tesser, M. Di Serio, M. Guida, D. Gaetano, A. Garcia Agreda, F. Cammarota, A comparison of different reactor configurations for the reduction of free acidity in raw materials for biodiesel production, Ind. Eng. Chem. Res. 46 (2007) 8355–8362.
[16] R. Tesser, L. Casale, D. Verde, M. Di Serio, E., Kinetics of FFAs esterification: batch and loop reactor modeling, Chem. Eng. J., in press, doi:10.1016/j.cej.2009.03.010.
[17] D. Siano, M. Nastasi, E. Santacesaria, M. Di Serio, R. Tesser, M. Guida, Method for forming a packing for resin catalytic packed beds and so formed packing, WO 2006/046138 A1 (2006).
[18] M.T. Sanz, R. Murga, S. Beltràn, J.L. Cabezas, J. Coca, Autocatalyzed and ion-exchange-resin-catalyzed esterification kinetics of lactic acid with methanol, Ind. Eng. Chem. Res. 41 (2002) 512–517.
[19] A. Fujii, S. Enomoto, M. Miyazaki, N. Mikami, Morphology of protonated methanol clusters: an infrared spectroscopic study of hydrogen bond networks of $H^+(CH_3OH)_n$ (n = 4–15), J. Phys. Chem. A, 01/02/2005–02/2005.
[20] D. Seguin, A. Montillet, D. Brunjail, J. Comiti, Liquid-solid mass transfer in packed beds of variously shaped particles at low Reynolds numbers: experimental and model, Chem. Eng. J. 63 (1996) 1–9.
[21] R.C. Reid, J.M. Prausnitz, B.E. Poling, The Properties of Gases & Liquids, 4th ed., McGraw-Hill, New York, 1987.